

# Gravity Level Dependency of Gas-Liquid Two-Phase Flow

Bu-Hong Choi<sup>†</sup>

(Manuscript : Received MAY 7, 2003 ; Revised MAY 14, 2003)

**Key words** : Gas-Liquid Two-Phase Flow, Microgravity, Flow Pattern, Void Fraction, Frictional Pressure Drop

## Abstract

More reliable design of thermal transport, power acquisition and thermal management systems requires the through understanding of the flow hydrodynamic, the differences and similarities between the two-phase flow characteristics of two-phase flow influenced by the gravity levels. The data of flow patterns, void fraction, frictional pressure drop associated with their characteristics were obtained at  $\mu g$ ,  $1g$  and  $2g$ . Flow patterns and void fraction data obtained at three gravity levels were compared with each other and previous models and correlations.

## NOMENCLATURE

	$\rho$	Density: [kg/m <sup>3</sup> ]
$C$	Chisholms parameter: [-]	Subscripts
$Co$	Distribution parameter: [-]	$G$ Gas-phase
$g$	Earth's gravity: [m/s <sup>2</sup> ]	$L$ Liquid-phase
$j$	Superficial velocity: [m/s]	$t$ Transition
$S$	Slip ratio: [-]	$T$ Total (gas+liquid)
$V_{Gj}$	Drift velocity: [m/s]	
$x$	Mass flow rate quality: [-]	
$X$	Lockhart-Martinelli parameter: [-]	

### Greek Symbols

$\alpha$	Void fraction: [-]
$\beta$	Volumetric fraction: [-]

## 1. INTRODUCTION

Two-phase loop systems using its latent heat capacity can meet the increasing power requirements and are well suited to thermal management systems of the

<sup>†</sup> Corresponding Author(Department of Mechanical Engineering, Kobe University, Japan),  
E-mail:choibuhong@hotmail.com, Tel:063)857-7849

future large applications, due to its abilities to handle large heat loads and to provide them at uniform temperatures regardless of the changes in the heat loads. A number of experimental works<sup>1)-4)</sup> have been conducted on gas-liquid two-phase flows at microgravity( $\mu g$ ) using flight or drop-tower. However, two-phase flow characteristics differ when subjected to earth gravity(1g), to hyper-gravity(2g), to Moon gravity, or to microgravity, due to the difference of buoyancy between two phases. Theoretical efforts<sup>5),6)</sup> to develop the two-phase flow pattern transition maps treating the gravity as a parameter have been presented. In order to design more reliable thermal management systems applying a two-phase flow, however, omnibus studies on the effect of gravity on the two-phase system factors are essential to the designers of such systems, because they are deeply inter-related.

Therefore experimental researches were performed on effects of gravity on the two-phase flow characteristics here. Some results are obtained from the experiments using MU-300 flight producing  $\mu g$  and 2g conditions and on ground with the identical flow conditions. The differences and similarities between the two-phase flow characteristics at three gravity levels are also discussed.

## 2. EXPERIMENTAL APPARATUS

The test flow loop shown in Fig.1 was used for collecting data at both  $\mu g$  and 2g during a parabolic trajectory flying of the

MU-300 aircraft, as well as at earth gravity conditions. Water and air are used as the working fluids. Water is forced by the gear pump from the separator tank, then it flows into the mixing section through the water flow meter, and eventually returns to the separator tank. Water flow rate is controlled by adjusting the rotational speed of the gear pump driven by an electric motor. Air is supplied from the compressed air cylinder, and passes through the sonic orifices and the air flow meter, then mixed with water in the mixing section. Air flow rate is controlled by passing the air through sonic orifices. The mixed air-water two-phase mixture exits the mixing section into the test section through the flow development section of 500mm length. The test section with water-filled viewing box for flow pattern observations is a transparent acrylic horizontal pipe of 10mm ID, 600mm length. The flow patterns are recorded by the high-speed video camera. The differential pressure drop is measured by the differential pressure transducers. The void fraction is determined by measuring the change in the electrical resistance as the amount of liquid contact with the void fraction probes changes.

The uncertainty associated with the void fraction measurements is estimated to be  $\pm 5.6\%$ .

The complete test flow loop system assembled with all the elements is installed in experimental racks, and then the racks are mounted in the MU-300 aircraft. The parabolic flight trajectories for producing  $\mu g$  and 2g environments are performed 57 times.

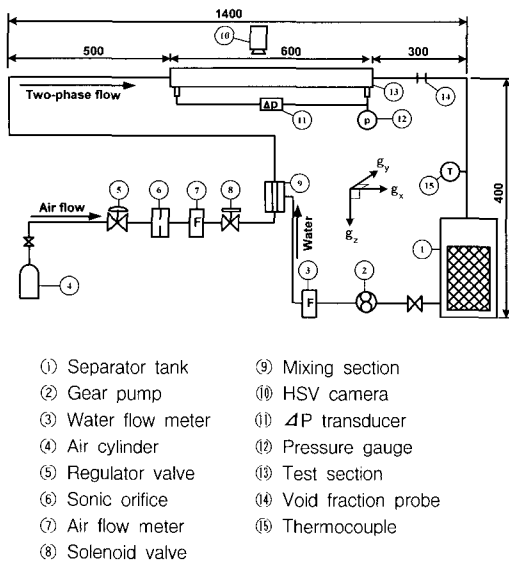


**Fig. 1 Schematic of test flow loop.**

### 3. RESULTS AND DISCUSSION

#### 3.1 Flow pattern transition

In the Fig.2, the flow pattern data obtained from microgravity experiments are plotted on the flow pattern map based on the gas and liquid superficial velocities, together with only the flow pattern transition results for 1g and 2g. The thicker-solid lines in the figure indicate the transition boundaries from one to another flow patterns for three gravity levels. It also shows the stratified flow region reduces, as the gravity forces reduce, however, the stratified flow do not exist at  $\mu g$ . All the transition boundary lines from bubbly to Taylor bubble flow (or plug flow) appear a positive slope of 1 meaning constant values of void fraction  $\alpha$ . The flow pattern transitions were found to occur at  $j_L=1.5j_G$  for  $\mu g$ ,  $j_L=5j_G$  for 1g, and  $j_L=7.5j_G$  for 2g, respectively. The values of the transition void fraction

$a_t$  in this region may be also calculated by using the drift-flux model ( $j_G/a=C\alpha j_T+V_{Gj}$ ) with the obtained experimental transition results. As the result, the values of the transition void fraction  $a_t$  of 0.392, 0.150 and 0.093 for  $\mu g$ , 1g and 2g were obtained, respectively. At  $\mu g$  conditions, bubbles are flowing with almost the same speed as the adjacent liquid phases, thus the probability of coalescence when bubbles contact each other decreases. This produces the result that the transition at  $\mu g$  in this region occurs at the higher void fraction value than that at 1g and 2g. It also implies that the gravity plays a significant role in the transition mechanism. For the transition from Taylor bubble (or plug flow) to slug flow, the transition boundaries in all the three gravity levels lied at the same line of approximately  $j_G=1.0m/s$ . For the transition from slug to semi-annular flow, the transition at  $\mu g$  occurs at the line of  $j_L=0.12j_G$ , while it occurs at  $j_G=3.7m/s$  for 1g,  $j_G=7.47m/s$  for 2g. As the magnitude of gravity is increased, due to the increase in buoyancy force, it becomes not only difficult to form the liquid slugs which bridge the tube, but also to reach at the maximum packing void value of  $a_{max}=0.5$  implying an upper limitation on the flow pattern transition. These lead to the result that the transition line for 2g lies at the higher  $j_G$  than that for 1g. In the transition from semi-annular to annular flow, the transition boundary lines for all the three g-levels are showed to be located at the same line of  $j_L=0.12j_G$ . It is the reason that the region is dominated by the inertia forces.

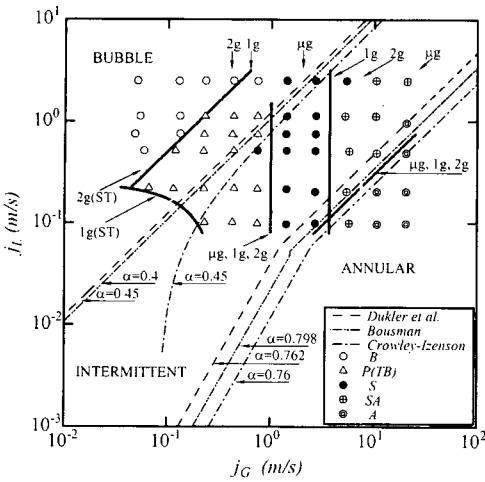


**Fig. 2 Flow pattern transition results at  $\mu g$ , 1g and 2g.**

As can be seen in the figure, the flow pattern transition results at three gravity levels are also compared with the models proposed by Dukler et al.<sup>1)</sup>, Bousman<sup>2)</sup>, and Crowley & Izenson<sup>5)</sup>, all for predicting the microgravity flow pattern transitions. These comparisons show a better agreement with Dukler et al. recommended the void fraction of 0.45 obtained from their experiments, for the transition from bubbly to Taylor bubble flow, and Bousman predicted with the void fraction of 0.798 for the transition from semi-annular to annular flow, respectively.

**3.2 Slip Ratio and Void Fraction**

The correlation between the cross-sectional average void fraction  $\alpha$ , slip ratio  $S$  and the volumetric fraction  $\beta$  [ $=j_G/(j_G+j_L)$ ] for three gravity levels is shown in Fig.3. As can be seen in the figure, when  $\beta > 0.5$ , the slip ratio  $S$  becomes over 1.0 meaning  $\alpha > \beta$  for  $\mu g$ , while when  $\beta > 0.15$  for 1g, and  $\beta > 0.1$  for 2g,  $S$  ranged over 1.0. From the above

results, it was found that the effect of gravity on the slip ratio decreased with the increase in  $\beta$ , and the difference of velocity between two phases in the range of  $0 < \beta < 0.5$  was very small for  $\mu g$ .

Comparisons of the void fraction values at  $\mu g$ , 1g and 2g conditions with the correlation proposed by Inoue-Aoki<sup>7)</sup> for vertical upward flow on earth gravity are shown in Fig.4 as a function of quality  $x$ . The solid lines in the figure indicate values of the void fraction  $\alpha$  calculated from the equation (1) for the quality  $x$  ranging from  $10^{-5}$  to 1.0.

$$\alpha = \left[ 1 + 0.025 \left( \frac{\rho_L}{\rho_G} \right)^{0.21} \left( \frac{1}{X} - 1 \right)^{0.25} + \left( \frac{\rho_G}{\rho_L} \right) \left( \frac{1}{X} - 1 \right) \right]^{-1} \tag{1}$$

As can be seen in the figure, it shows the void fraction values generally increase, as the quality  $x$  increases. The difference between void fraction data and the correlation gradually decreases, thus it shows very good agreement with each other with the difference within  $\pm 3.7\%$  for annular flow region for all three gravity levels. It also indicates the increase in void fraction with the reduction of gravity. It could be perhaps due to the reciprocal multiplication of the following two causes. One is a size of bubbles detached from the surface on mixing section. In the laminar flow region at  $\mu g$ , since surface tension plays a larger role on the bubble than buoyancy and turbulence forces, then the time lag of bubble staying on there increases, and consequently the size of bubble at  $\mu g$  when detached from there becomes larger than at the gravity fields.

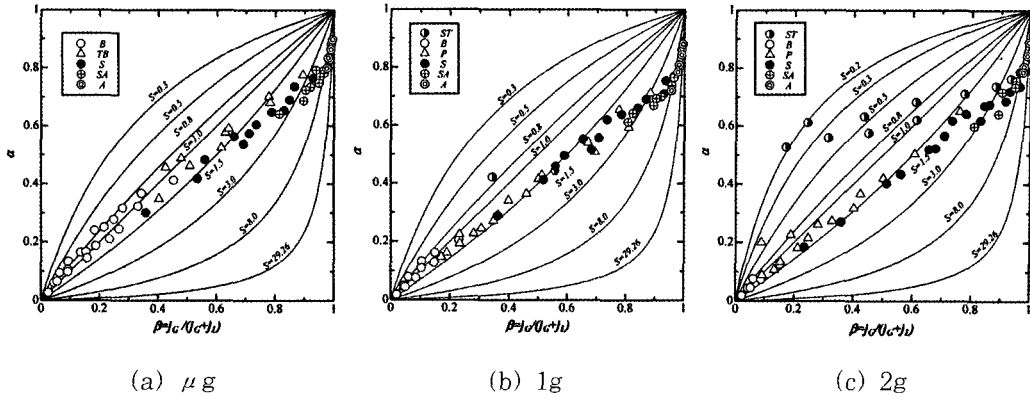


Fig. 3 Correlation of void fraction  $\alpha$  at microgravity with volumetric fraction  $\beta$  related to slip ratio  $S$ .

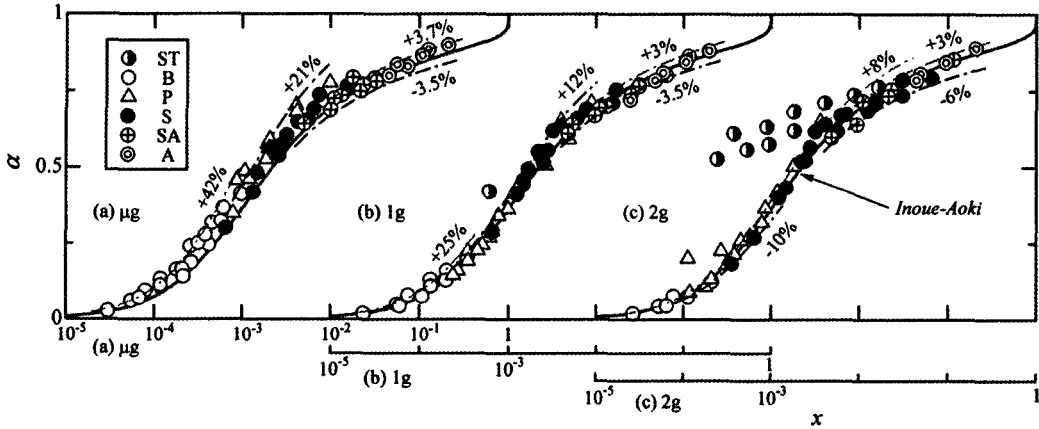


Fig. 4 Comparisons of void fraction  $\alpha$  at  $\mu g$ ,  $1g$  and  $2g$  with Inoue-Aoki model.

The other is a configuration of bubbles in the tube. When the gravity is reduced, bubbles have more symmetrical distributions, thus they receive uniformly surface tension from the surrounding liquid phases, consequently almost spherical configurations with the size as much as the tube inside diameter. Even on the annular flow region at high flow rates, the figure also shows slightly higher void fraction value at  $\mu g$  than at gravity fields. It could be due to the effect of the capillary force when used a small tube in

diameter as this study.

### 3.3 Frictional Pressure Drop

The ratio between frictional pressure drop values at  $\mu g$  and  $1g$  is shown in Fig.5 by using the Lockhart-Martinelli parameter  $X$  defined in the equation (2).

$$X = \left[ \frac{(dp/dz)_L}{(dp/dz)_G} \right]^{0.5} \tag{2}$$

where  $(dp/dz)_L$ ,  $(dp/dz)_G$  are the single-phase liquid and gas frictional pressure gradients calculated using the liquid and

gas flow rate alone, respectively. The figure shows that the maximum ratio of the frictional pressure drop at 1g to that at  $\mu g$  is approximately 1:1.3 for the region of  $j_L \leq 0.2m/s$ . while it shows no significant difference for the turbulent flow region of  $j_L \geq 0.5m/s$ . However, the experimental result is to be unexpected. In general, if the slip ratio is reduced, then the interfacial friction factor should be also reduced, and consequently the pressure drop should be rather smaller. However, the unexpected result could be explained by the reason that the frictional pressure drop might be influenced more strongly rather by the difference in the flow pattern induced by the change in gravity than by the difference in the slip ratio. It is namely the reason that for bubble and Taylor bubble flows at  $\mu g$ , the velocity of the liquid phase between the tube wall and bubbles is accelerated due to the bubble or Taylor bubble traveling along the tube centerline with nearly the same size to the tube inside diameter, although those at 1g and 2g move along the upper wall. Moreover, even on the same annular flow region, the significant differences are occasionally showed. It could be due to the influence of the difference in the phase distribution in a conduit, thickness and surface roughness of the annular liquid film, it should be more fully studied on those in future.

Comparisons between 1g and 2g follow generally the same trend, as can be seen in the Fig.6. although the resulting reasons were different from those between  $\mu g$  and 1g. Comparisons of the movie films on the stratified and plug flows at 1g

and 2g confirmed that the stratified flow at 2g has a lower liquid phase in depth and a rougher interface, as well as the plug flow at 2g has a longer gas plug in length and a rougher interface, as respectively compared to such flow patterns at 1g. In case of the stratified flow at 2g, the increase in the velocity of the liquid phase in the reduction flow area causes the wave amplitude in air-water interface to increase, consequently frictional pressure drop to increase. These would produce the difference between frictional pressure drop values at 1g and 2g stratified flow. Comparisons for the plug and slug flows at 1g versus the stratified flow at 2g show significant difference. This may also be due to the influence of the roughness in the interface by the accelerated liquid phase, judging from the fact that the difference in the ratio differs by the difference in the degree of the roughness on the interface, even on between 1g and 2g plug flow. However it should be also noted that the roughness might be induced by the flight its vibration and the residual g-levels during flying. The maximum ratio of the frictional pressure drop at 1g to that at 2g is approximately 1:1.45.

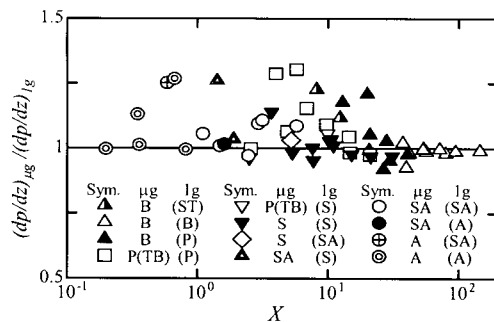
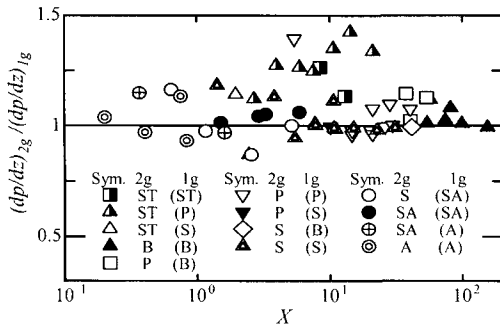


Fig. 5 Comparison between frictional pressure drops at  $\mu g$  and 1g.



**Fig. 6 Comparison between frictional pressure drops at 1g and 2g.**

#### 4. CONCLUSIONS

In order to investigate the gravity dependency of two-phase flow, several experiments were performed at  $\mu g$  and  $2g$  on board MU-300 flight, and at earth gravity. The results obtained in this study are as followings:

1. The slip  $S$  reduces and void fraction  $\alpha$  increases with the increase in gravity level.
2. The maximum ratio of the frictional pressure drop at  $1g$  to that at  $\mu g$  was about 1:1.3. It was due to the difference between the flow patterns at  $1g$  and  $\mu g$ .
3. The frictional pressure drop at  $2g$  was greater than that at  $1g$  by 45%. It may be due to an increase in the roughness of air-water interface induced by the accelerated liquid phase at  $2g$ .

4. In the laminar region, the effect of the gravity level on the flow pattern transition and the frictional pressure drop was relatively significant.

#### REFERENCES

- [1] Dukler, A. E., et al., Gas Liquid Flow at Microgravity Conditions: Flow Patterns and Their Transitions, *Int. J. Multiphase Flow*, 14, pp389-400, 1988.
- [2] Bousman, W. S., Studies of Two-Phase Gas-Liquid Flow in Microgravity, *NASA Contractor Report 195434*, (1995), pp85-228.
- [3] Zhao, L., Rezkallah, K.S., Pressure Drop in Gas-Liquid Flow at Microgravity Conditions, *Int. J. Multiphase Flow*, 21, pp837-849, 1995.
- [4] Choi, B., et al., A Study of Gas-Liquid Two-Phase Flow in a Horizontal Tube under Microgravity, *Ann. NY. Acad. Sci.*, 974, pp316-327, 2002.
- [5] Crowley, C. J. and Izenon, M.G., Design Manual for Microgravity Two-Phase Flow and Heat Transfer, *AL-TR-89-027*, pp1-49, 1989.
- [6] Reinarts, T. R., Adiabatic Two Phase Flow Regime Data and Modeling for Zero and Reduced (Horizontal Flow) Acceleration Fields, *Ph. D. Dissertation*, pp25-252, 1993.
- [7] Akagawa, K., Gas-Liquid Two-Phase Flow, *Corona Publishing Co. Ltd.*, 36-72, 1974.